Open Hardware: Towards a Fully-Wireless Sub-Cranial Neuro-Implant for Measuring Electrocorticography Signals

January 11, 2016

David Rotermund [1,*], Jonas Pistor [2], Janpeter Hoeffmann [2], Tim Schellenberg [3], Dmitriy Boll [4], Elena Tolstosheeva [4], Dieter Gauck [5], Dagmar Peters-Drolshagen [2], Andreas K. Kreiter [5], Martin Schneider [3], Steffen Paul [2], Walter Lang [4], and Klaus R. Pawelzik [1]

[1]University of Bremen, Institute for Theoretical Physics, Bremen, Germany
[2]University of Bremen, Institute of Electrodynamics and Microelectronics, Bremen, Germany
[3]University of Bremen, RF and Microwave Engineering Laboratory, Bremen, Germany
[4]University of Bremen, Institute for Microsensors, -Actuators and -Systems, Bremen, Germany
[5]University of Bremen, Institute for Brain Research, Bremen, Germany

Corresponding Author:
David Rotermund, University of Bremen, Institute for Theoretical Physics, Hochschulring 18, Bremen, 28359, German, davrot@neuro.uni-bremen.de

Abstract

Implantable invasive neuronal interfaces to the brain are an important keystone for many interesting future medical applications. However, entering this field of research is difficult since such an implant requires components from many different fields of technology. Beside the required amplifiers, analog-digital-converters and data processing, the complete avoidance of wires is important because it reduces the risk of infection and prevents long-term bio-mechanical problems. Thus, means for wireless transmitting data and energy are also necessary.

We present a module, containing the necessary components for wireless data transfer and inductive powering for such implantable neural systems, and its base station. They are completely built of commercial off-the-shelf (COTS) components and the design files are available as Open Hardware / Open Source. The data is transmitted via Microsemi ZL70102 transceivers and custom Tx/Rx antennas for bidirectional communication using frequencies in the MICS band, with a maximal data rate of 515 kbit/s. The energy is transmitted via a wireless inductive energy-link based on the Qi standard. On the implant site a handwound litz wire coil harvests energy from the magnetic field and delivers, over a short distance, more than enough inductive power to the fully implantable unit.

Based on this wireless module we also present a fully wireless neuronal implant for simultaneously measuring electrocorticographic (ECoG) signals at 128 locations from the surface of the brain. The implant is based on a flexible printed circuit board and is aimed to be implanted under the skull.

The application-specific integrated circuit (ASIC) was designed in-house and allows to adapt the data processing of the implant to changing user-defined parameters.

1 Introduction

There is nothing more drastic in a person's life than losing the control over the own body (e.g. by a neuro-degenerative disease, stroke, paraplegia), getting blind or losing limbs. The actual state of medical technology has very limited options for helping this group of people. Results from brain-research suggest that it should be possible to build technical medical devices which interact with the neuronal activity patterns of the brain to ease the loss of life quality and partially restore the lost functionality (e.g. creating visual perception [Schiller and Tehovnik, 2008, Dobelle, 1999, Schmidt et al., 1996] and extracting information from neuronal activites [van Gerven et al., 2009, Andersen et al., 2010, Lebedev and Nicolelis, 2006, Ifft et al., 2012]). Even with the knowledge of today, astonishing assisting systems for this group of people are possible [Wang et al., 2013, Hochberg et al., 2006, Simeral et al., 2011, Dobelle, 1999]. One important example are invasive brain-computer interfaces (BCI), which allow to control computers or robot-arms by evaluating the actual spatio-temporal brain activity patterns (e.g. [Lebedev et al., 2011, van Gerven et al., 2009, Lebedev and Nicolelis, 2006, Andersen et al., 2010, Velliste et al., 2008, Wang et al., 2013, Hochberg et al., 2006, Musallam et al., 2004, Moran, 2010] and many more).

Transferring such systems into the daily medical routine remains a highly challenging task. One major problem is the interface which aquires signals directly from the brain. This interface needs to be long-term stable (up to several decades), bio-compatible, and persistent against humidity surrounding the implant in the form of brain liquor. From a functional point of view these systems need to provide a high spatial- and temporal resolution to measure and/or change the neuronal activity patterns in the human brain.

For an invasive BCI application, the required neuronal data needs to capture these patterns with highest possible temporal and spatial resolution, with as few as possible signal distortions, such as band-pass filtering of the signals by bones, fat, and skin tissues. This requires data recording as close as possible to the nerve cells, which is antagonized by the medical demands of safety and long-term stability. An applicable compromise is to use electrocorticography (ECoG) signals, recorded from the surface of the brain or the dura matter, which still contain detailed information usable for BCI [Rotermund et al., 2013, Schalk, 2010, Pistohl et al., 2012, Pistohl et al., 2008, Brunner et al., 2011, Leuthardt et al., 2004].

To achieve such functionality of modern neuroprotheses, complex data analysis procedures need to be applied in real time [Rotermund et al., 2013, Rotermund et al., 2006, Andersen et al., 2010, Wu and Hatsopoulos, 2008, Li et al., 2011]. At the moment, it is not possible to perform this computationally extensive data processing with processor units placed inside the human body. The main reason lies in the high amount of heat produced by the processors which is highly constraint for such an implant [Silay et al., 2008, Kim et al., 2007a, Kim et al., 2007b]. As a result, the collected data has to be transmitted to an external analysis system. In order to reduce the inherent risk [Voges et al., 2006, Lee et al., 2000, Nair et al., 2008] of infection, cerebral fluid loss, as well as bio-mechanical problems in chronic applications, the implant must not be wire-bound to a base station. Hence, all components of the implant need to be located inside of the human body. It would be even more advantegeous if the implant can completely be placed under the human skull. Following this requirements, the system has to be capable of transmitting data wirelessly between an external base station and the implant side, as well as providing energy for the implant through a wireless power link.

Although there are approaches for wireless data [Asgarian and Sodagar, 2011] (using various technologies, e.g. Ultra Wide Band [Chae et al., 2009], Offset Quadarture Phase Shift Keying [Liu et al., 2009],

Amplitude Shift Keying [Navaii et al., 2012], Frequency Shift Key Modulation [Borton et al., 2013], RF Backscattering [Schwerdt et al., 2011] and RF ID Technology [Aubert, 2011]) and energy transmission systems [Olivo et al., 2011, Rapoport et al., 2012, Ho et al., 2014], especially for neuronal implants, these systems are not available on the market. Thus, it is nearly impossible for other groups to obtain and (re)use these systems. We would like to support other researchers in the field by providing them with a working wireless energy- and data interface, and thus push their research and enable them to focus on other functional parts of their system. Therefore, we developed a module that is based on commercial off-the-shelf (COTS) components. Our actual system can be used for experiments with animals. In the long run, we aim at a system for human medical applications. The presented wireless module incorporates two connected sub-segments: one to supply wirelessly the implant with energy and the other one for wireless communication.

Based on this Open Hardware wireless module and its base station, we started to develop a neuro-implant which had to be sub-cranially implanted. The typical prototype system of a neuronal implant (e.g. [Borton et al., 2013, Yin et al., 2012, Aceros et al., 2011]) consists of two parts. One set of components is located under the skull, connected via cables to a second set of components outside the skull (e.g. head or torso). Another approach is to replace parts of the skull with the implant [Charvet et al., 2013] or components of the external basestation [Muller et al., 2014]. First prototypes of fully implantable systems were developed, based on the Utah needle array [Sharma et al., 2011, Harrison et al., 2009, Kim et al., 2009, Harrison et al., 2008]. However, they were mainly taylored for recording the timing of action potentials and not of ECoG signals. Also it is not yet clear if the approach with these needle arrays will work over several decades [Barrese et al., 2013]. Some systems even contain rechargeable batteries [Hirata et al., 2011] which are charged via an inductive link. Such a battery has a limited lifetime which is below several decades. In this context, one major problem of neuro-implants, in comparision e.g. to pacemakers, is that after some time scar-tissue or even bone encapsulates the part of the implant situated within the head. Without damaging the brain tissue, replacing the implant or parts of it (e.g. batteries) becomes very problematic. Ascribing a very high importance to long-term stability and safety, it is highly desirable and advantageous to keep the natural barrier, established by a completely closed skull, against germs and cerebral fluid leakages [Voges et al., 2006] intact and avoid the use of energy storage elements with a limited lifetime.

In 2010 we started to design an application specific integrated circuit (ASIC) [Pistor et al., 2011] which was able to communicate with the analog-digital-converter on the Intan Tech biosignal amplifier RHA 2116 for collecting electro-physiological data. Later we improved this ASIC design by upgrading it with support for the presented wireless module ([Pistor et al., 2013, Tolstosheeva et al., 2013]). Those first prototypes were based on large and fully rigid FR-4 PCBs. Since the ability of the implant to snuggle against the brain is important [Tolstosheeva et al., 2011], we finally integrated all components on an industry grade flexible PCB-foil. Beside the presentation of the wireless module and its basestation we will report the results of this latest improvement in the following.

2 Results

2.1 System concept

The intention behind our approach was to build a system that can completely be implanted sub-cranially, which is supplied with energy via a wireless link (without any implanted batteries) and which exchanges data wirelessly with an external base station. Fig. 1 shows the functional blocks necessary for such a system.

An array of electrodes serves as an interface between the brain tissue and a set of integrated analog signal amplifiers with band-pass properties. After the amplification of the neuronal signals, analog-digital

converters digitize the incoming signals and generate several digital data streams. An Application Specific Integrated Circuit (ASIC) filters these data streams according to user-defined specifications and merges the parallel streams into a single one, optimized for a minimal bandwidth. The condensed data stream is re-packed into transmission packages and transmitted via an RF transceiver data link to an external base station. The base station receives the data packages and unpacks, checks, and repacks them. These newly built packages, optimized for fast processing by 32 or 64-bit CPUs, are sent via Ethernet to an external PC for further use (e.g. visualization and analysis). From the external PC, the base station receives instructions about the user defined parameters for the data processing of the implant and transmits them to the implant to set the desired configuration in the ASIC. Beside the bi-directional wireless data exchange, the implant collects energy from an inductive wireless power link for power supply.

2.2 Realization of the wireless module

The presented wireless module incoperates two connected subsegments: One which supplies the implant wirelessly with energy and the other one for wireless communication. Fig. 2 visualizes all the necessary components plus its external counterparts. Fig. 3 shows a PCB realization of that block diagram with a total size of 20 mm x 20 mm x 1.6 mm. In the following section, both functional blocks are described in detail.

The power supply: The concept of the wireless power link was designed based on the Texas Instruments (TI) bqTESLA system [TI, 2011]. TI created these products for wirelessly recharging mobile devices, e.g. MP3-players and smartphones, based on the QI standard. Consequently, the corresponding components - designed for an integration into a mobile device - are highly miniaturized and designed for high efficiency. In theory, this link can deliver up to 5 Watt [TI, 2010]. Between the energy receiver and transmitter an ongoing communication regulates the properties of the wireless energy link dynamically and load-dependently. The frequency of the power link is dynamically regulated between 110 kHz and 205 kHz [TI, 2010] and depends on the consumed power on the secondary side (implant). This regulation, in combination with a fixed resonance frequency of the receiver, helps to prevent harvesting too much energy on the implant site, that could lead to chronic heating.

On the primary side (base station) we used the bqTESLA wireless power evaluation kit (bq25046EVM-687) as a low-cost power transmitter [TI, 2010]. On the secondary side, a BQ51013YFFT IC as power receiver is part of the design [TI, 2012]. This chip-sized ball grid array (BGA) contains the means to communicate with the external transmitter, rectification of the inducted AC wave, and voltage regulation. The receiver IC delivers a 5V power rail. If this IC is used, then two important design aspects have to be considered: 1.) Many of the required ceramic capacitors on the side of the secondary coil need to be rated for 50V. As a result, the capacitors with larger capacitance are too thick for some target areas of implantation. Therefore, it is necessary to split them into several smaller parallel capacitors. 2.) Due to the small distance between the balls of the BGA, it was not possible to contact important pads in a normal fashion. Thus, it is necessary to place *via* holes underneath the pads for the BGA package. This requires the *via* to be filled and closed with a planar surface, which is quite demanding for the (external) manufacturer of the printed circuit board (PCB). Examples based on 150m thick FR4 and a 50m thick flexible PCB-foil substrate were tested successfully. However, due to the required very fine resolution (50 µm strip width and distance between elements) of the PCBs, most of the flexible PCB-foils were produced with faults (e.g. shortcuts). Fortunately, we were able to fix some of them by manual cutting and grinding.

For the secondary side, we used a handwound coil (see figure 3) with 20 mm x 20 mm size and 18 turns of litz wire (20 x 0.05 mm individual wires). For the power-receiver IC we used, the maximum distance is defined by the Qi standard with 5mm. This requires that the secondary coil is placed between skin and skull with two thin wires through the skull. With our transmitter we are able to bridge a distance of 4.5mm with the described coil (L=10.5uH, Q=1). With a modified receiver coil we reached 5.5mm

Component	power consumption
Zarlink ZL70102 transceiver	17mW (measured)
ASIC	up to 9.44mW (measured)
Clock quartz	16.5mW (measured)
RHA amplifier arrays	5mW (each IC) (measured)
DCDC-Converter	8.5mW (for 1 RHA), 15mW (for 8 RHAs), (datasheet)
TI inductive power receiver	10-40 mW (datasheet)

Table 1: Estimated power consumption of the implant's components.

(L=15uH, Q=0.76). Fig. 4 shows results of a range measurement, and how the base station adjusts the field strengh and frequency depending on the distance and the inductance of the receiver coil. The figure shows no significant difference in the operation point (frequency and voltage) between air and meat as transmission medium. The received rectified power was set to 100mW for the experiment. In the near future, new power receiver ICs based on the updates Qi standard [WPC, 2014] (which is claimed to be backwards compatible with the existing receivers and reach distances between 12mm and 45mm) as well as the 'Rezence' standard from the alliance for wireless power can be expected. These new standards are based on magnetic resonance which are designed for much higher distances of several cm while allowing obstacles between the primary and secondary coil. It is expected that an update of our implant to these new standards will allow to place the secondary coil also under the skull.

The 5V output of the receiver IC is too high for operating the RF transceiver and other active components. Thus, a highly efficient and very small DC/DC converter is required. We applied a Torex XCL 206 step-down micro DC/DC converter with built-in inductor which only requires two small capacitors as external components [Torex, 2011]. In the expected operating point, it works with a efficiency over 80%. Due to its switching nature, PI filters are advised on the consumer side. However, additional capacitive loads exceeding 50F cause problems and loads beyond 70F stopped the DC/DC converter from working. An estimate for the main electrical loads of the components of the implant are shown in table 1. Combined with the losses of the power supply ICs, the fully equipped implant will dissipate about 110mW-140mW of power, while the intensively tested prototype with one RHA consumes about 73mW-103mW (both are presented in the next section). For safety reasons, the power receiver IC is programmed not to accept more than 200mW to limit the heating in case of failure.

Data Transfer: The wireless data transfer is based on Microsemi ZL 70102 transceivers [Microsemi, 2010]. The RF transceiver operates in the Medical Implant Communication Service frequency band (MICS, 401 - 406 MHz) and is commercially available for medical applications including implants. The transceiver establishes a bi-directional wireless link, using 4-FSK or 2-FSK mode of operation. In order to achieve a high data rate, especially for a continuous data streaming, it is necessary to provide a large extra memory for the controller, who is operating the transceiver via SPI on the implant site. This is necessary because pauses of unknown origin in the data transfer of up to 80 ms may randomly occur. The transceiver is available as a chip-sized BGA.

We measured data transfer rates with the implant prototype in wireless operation (Fig. 5). For the measurement we configured the implant to sample 52 channels at 2kHz and a resolution of 10 bits, which generates a data stream on the implant with 1.12 Mbit/s while the Zarlink transceiver shows a limitation of 515 kbit/s. This guarantees a full TX-buffer and allows to measure the maximal transmission performance. For each measurement condition (medium and distance), a set of 10 data tracks was recorded, each containing 100,000 sample sets. The duration of the transmission for each set was measured to reach the transmission rate.

For simulating in-vivo-measurements, we placed the implant prototype between two 1 cm thick stacks of sliced meat. We also tested the implant in air and observed comparable transmission rates at similar

distances. Most important is the result, that the data can be transmitted with almost maximum transceiver speed through 10mm of meat. A data transmission was possible up to 47 mm, but with a strongly reduced data rate due to the retransmission of corrupted packets. Also under good conditions some samples are lost, because the Zarlink transceiver is not optimized for real time transfer but for good data integrity. Timestamps are included by our implant electronics to reconstruct the timing, even if packets are lost.

The ZL70102 requires several external components. Among those is a 24 MHz clock. We used a very small (2 mm x 1.6 mm x 0.7 mm) CMOS 3.3 V clock from NDK (NZ2016SA) [NDK, 2013]. Besides driving the transceiver, it also provides a clock signal for other components (e.g. ADCs, microcontroller, FPGAs or ASICs (e.g. [Hoeffmann et al., 2012]) for data processing).

Between the RF transceiver and the antenna (circular loop antenna with 5mm diameter), we installed an adaptive antenna-matching circuit with a SAW filter (RF Monolithics RF3607D, 403.5 MHz SAW filter) [RFMonolithics, 2010]. The adaption of the matching circuit is accomplished by using two tunable capacitors which are part of the ZL70102. Those are optimized by the transceiver automatically. The SAW filter is one of the largest components (3.8 mm x 3.8 mm x 1.0 mm) on the implant.

For the base station parts outside the body, a solution based on a Microsemi ZL70120 is used [Microsemi, 2013]. Among other components, this RF transceiver base station module contains a ZL70102, antenna-matching circuit and a clock. We designed a simple PCB for this module and added a 50 Ohm rectangular loop antenna to it (see Fig. 6). Via SPI, we operated this transceiver base station module with a FPGA using a custom firmware. This FPGA is part of a board (Orange Tree ZestET1) with Gigabit Ethernet connectivity [OrangeTreeTechnologies, 2013]. This allowed us to stream the data from the implant to an external PC via TCP/IP. The base station also supplies the implant with control sequences from the PC using the other direction of communication.

2.3 Realization of the implant prototype

The described system for the implant was realized (see Fig. 7) with 128 gold electrodes in an area of 9mm x 17mm with a diameter of 0.4mm for the individual electrodes and a center-to-center electrode distance of 1.4mm on a flexible 50µm thick PCB-foil (DuPont Pyralux AP). This PCB-foil has a size of 34mm x 79mm. It can be folded at 3 lines (see Fig. 8) to further reduce the overall size of the implant as shown in Fig. 9. All electrical components are placed on one side of the two-layered PCB-foil with respect to the polyimide process developed for future implementations. The weight of the implant is 1.72g, and it fits into a volume of 4mmx24mmx32mm without the power-link coil. The coil has a square shape with a side length of 22mm and a thickness of 2.2mm. Due to problems with the quality of the PCB foils, the implant prototype used for testing was equipped with only one instead of all 8 amplifier arrays. This has an effect on the power consumption (each RHA array consumes 5mW in this scenario) and consequently to the number of available channels for measurements. For testing the different configurations, the 16 available measurement channels can be combined with the internal RHA test pattern generators in our ASIC. Besides the missing RHA arrays, the prototype supports all functions of the final implant, especially the complete wireless power and data transmission. First tests of the electronics, in a non-implanted state, were already conducted in an animal experiment as well as long-term in-vivo tests of implanted electrodes [Tolstosheeva et al., 2011].

For the analog front-end Intan RHA2116 chips are used, which include the neural amplifiers and an analog-to-digital converter (ADC). Eight of these ICs are part of one implant, where each RHA provides 16 analog channels. The RHA contains, beside bio-signal amplifiers with a band-pass filter, an ADC that allows sampling all its individual channels at 10 kHz and 16 bit resolution. The integrated ADC is documented in a previous version of the RHA2116 data sheet. We chose to operate the ADCs with their full 10 kHz sample rate which allows to reuse this setup with intracortial electrodes for recording action potentials. These ADCs generate 8 parallel data streams with a total of 20.48 MBit/s.

Resource	Usage (RHA)	Usage (RHD)
CORE	5859 of 6144 (95%)	5236 of 6144 (85%)
IO (W/ clocks)	38 of 68 (56%)	38 of 68 (56%)
GLOBAL (Chip+Quadrant)	6 of 18 (33%)	6 of 18 (33%)
PLL	0 of 1 (0%)	0 of 1 (0%)
RAM/FIFO	8 of 8 (100%)	8 of 8 (100%)

Table 2: Usage of the IGLOO nano FPGA resources for an implant with Intan RHA or RHD analog front-end. A large portion (up to 33% in the case with RHAs) of these core resources are used by strutures for simulation of the functionallity of analog front-ends for testing purposes.

On the other end of the data processing chain, the RF transceiver is only capable of transmitting up to 0.515 MBit /s.

The 8 ADC data streams are collected by an in-house designed digital ASIC [Pistor et al., 2013]. Besides serializing these parallel inputs, the ASIC has the capability to significantly reduce the incoming data according to user-defined parameters such as sample rate, resolution and the selection of electrodes which are included in the recording. Since the performance of the implanted electrodes can degrade with time, all the parameters can be changed dynamically during runtime in order to utilize the limited RF data bandwidth in an optimal way. Thus the implant uses the bi-directional nature of the RF link for receiving user-control commands from the base station during operation. The ASIC also controls the RF transceiver (e.g. initializing the connection and its parameters) as well as provides and caches the outgoing data (embedded into a suitable and compact transmission protocol) for achieving a high and continuous data transmission rate via the SPI connection. Furthermore, the ASIC contains integrated testpattern generators, which can be used instead of the real measurement data from the Intan RHA2116 ICs.

Taking the data processing structures from the ASIC, we reimplemented the design in a way suitable for Microsemi IGLOO AGLN250 nano field programmable gate arrays for providing a complete neuro-implant development system. Besides implementing the firmware for the Intan RHA analog-front end, we also updated it for the use of the newer Intan RHDs. Table 2 shows the required resources on the FPGA. The bare die of the FPGA is slightly bigger (3.22mm x 3.48mm) compared with the ASIC. However, this component is still small enougth to be used on a neuro-implant development system with the same size. In future designs of our implant development prototype, the nano FPGA will allow us to develop and test new versions of the data processing while keeping the test system in realistic dimensions. We provide the RHA and RHD based nano FPGA firmwares as Open Source.

2.4 Thermal stress for the tissue

Tissue Heating: A major concern for neural implants is the heating of the tissue, as proteins start to denaturate at approximately 40°C. The IEEE Standard [IEEE, 2006] states a brain temperature 40.5°C as critical for a heat stroke. The tissue temperature close to the implant is affected by different heat sources. Most criticial is the joule heating of the implant electronics due to the high power densities (e.g. 17mW in $9mm^3$ for the transceiver IC). Due to the folded structure of our implant, all active components are embedded inside the implant, which strongly increases the contact area to the tissue.

Another heat source are eddy currents from the inductive field of the power and data transmission in the conductive tissue and in the implant. The eddy currents are expected to be negligibly small, according to the stable operating point shown in Fig. 4. Heating by the field of the data transmission in the MICS-band can also be neglected. The whole RF transceiver only comsumes 17mW of power, only a percentage of it is really transformed into field energy.

Finally the joule heating of the base station coil, which has contact to the skin above the implant, increases the temperature of the tissue. A simple countermeasure could be the cooling of the base station.

Simulation of joule heating: As our prototype is equipped with only one amplifier array instead of eight, we used a simple FEM model (COMSOL) to evaluate the heating of the final, fully assembled and folded implant. We used the outer dimensions shown in Fig. 9 and applied a heat source of 100 mW distributed over the volume of the implant. We chose 100mW for the simulation as an estimation for the typical power dissipated by a fully equipped implant in operation. Actual values might be lower or higher depending on the number of active RHAs and the actual efficiency of the TI inductive power receiver, but they do not change the magnitude of the resulting temperatures. Fig. 10 shows the heatup curves at the surface of the implant and at different distances within living tissue. The temperature at the surface in thermal equilibrium is calculated to be 0.25K above the starting temperature of 37°C, in a sphere with 10cm diameter and a border temperature of 37°C. Additionally, Fig. 11 shows a temperature map taken after 300 seconds, with the 24mm x 4mm cross section of the implant positioned in the center.

Measurement of total heating for the prototype: In addition to the simulation, we made an experiment to observe the heating in wireless operation. The measurement setup is shown in Fig. 12. The implant prototype was isolated with a thin PCB-foil of plastic wrap against a liquid medium (Ringer solution) with a volume of 150ml. For the temperature measurement we used a thermocouple with contact to different parts of the implant. Based on the simulation, we expected the surface temperature to be saturated after a few minutes. As longer periods of activity will not provide meaningful results, because in contrast to a living subject, the surrounding tissue (in our case 150ml fluid) would heat up more and more because of the small volume and lack cooling by blood perfusion.

Different measurements were taken in the Ringer solution with contact to different spots at the implant. The black curve in Fig. 10 shows a rapid joule heating of the coil in air, while the heating saturates at approximatly 0.1C in water (red) and even below in the conductive Ringer's solution (yellow). Close to the ASIC, which is covered under a 0.75mm plastic housing and has a power dissipation of 9.44mW, we also measured a temperature increase below 0.1°C.

In contrast to the low heating at the ASIC, the blue curve shows the temperature on top of the uncapsulated RF transceiver IC, which has a power dissipation of 17 mW. In Fig. 9, the transceiver is located behind the saw filter, which is ca. 1mm higher than the transceiver IC. Thus, after folding, the transceiver IC has no direct contact to the tissue. In our experiment, the PCB-foil was not folded and we saw a strong temperature increase at the contact between the IC and the liquid medium. The ground planes in the substrate are expected to distribute the thermal power equally to the outer implant surface.

2.5 Noise of the analog front end

For a rms-noise test, we analyzed the signals from a measurement, where the electrode array of the implant prototype was placed in Ringer solution (Fig. 13). The prototype implant with one RHA was working in wireless operation, sampling 16 channels with 1kHz and a resolution of 10 bits. Since many of the externally produced PCB-foils had defects, we decided to use a repairable sample with only one Intan RHA2116 chip with 16 working channels. The rms noise of the measurement is 7.9µV. Fig. 14 shows the spectrum of the system noise. Figure 15 shows what sinusoidal waves look like when recorded with the analog front end of the implant.

3 Discussion

Wireless module: We presented an open hardware module for wirelessly exchanging data between an implant and a base station as well as providing a wireless power link for the implant. Furthermore, we introduced the components for a corresponding external base station. These designs are purely based on COTS components. We provide the complete design as open hardware project to give future researchers in this field a proper starting point for their developments. In this way, we hope to inspire new ideas in the field of neuro-implants.

For the future, we plan to improve two aspects of the implant module: 1.) By exchanging the power harvesting to magnetic resonance technology (the new Qi standard or the Rezence wireless power charging standard), we intend to increase the maximal operating distance between the primary and secondary coil. In the actual state our implant requires an energy harvesting coil between the skin and the skull which is connected with two small wires to the implant under the skull. 2.) The effective data transmission rate is limited to 515kbit/s. For many applications this transmission rate is too low. We plan to develop and add optical data transmission channels for future designs.

In addition *in vivo* tests have to be performed in order to verify the system performance under real measurement conditions. We need this information to estimate the development steps that have to be taken for making the system safe enough for using it for human patients.

Overall implant: Based on the wireless module, we have presented a system concept and its implementation of a fully wireless sub-cranially implantable system for measuring ECoG signals at 128 positions on the surface of the brain. The system, targeting medical and neuro-prosthetic applications, consists of in-house designed and off-the-shelf components bonded to a flexible board.

For development purposes, we also present two versions of firmwares for the Microsemi Igloo nano FPGA and provide them as open source. These firmwares are based on the implant's ASIC. One was written for the Intan's RHA. The other one was optimized for the newer Intan RHD analog front-end. With this nano FPGA a development version of the whole implant can be built entirely from off-the-shelf components.

Ex-vivo tests proved the feasibility of our approach. However, first short term in-vivo tests revealed a problem when the reference electrode path has a high impedance connection. In this case, the recorded signal is strongly reduced in its amplitude and the neuronal signal nearly vanishes from the recorded time series. The reason for this behaviour is not fully understood yet. One hypotheses is that this configuration allows the wireless power supply to induce an addition 100KHz sinusoidal signal on top of the neuronal signal. These combined signals are now larger than the threshold voltages of the ESD protection diodes of the input channels of the RHA. As result the protection diodes open a direct connection to electrical ground which eradicates the signal. A larger distance between the RHAs and the energy transmitter / energy harvesting coil may reduce the problem or switching to a different kind of wireless energy link system might also remove this problem.

Another main remaining obstacle preventing us from applying the system in-vivo, are long-term stable biocompatible coatings which can protect the electronics from the harsh environment in the body. This coating has to stay intact over many years and has to be very thin and flexible. We designed the implant to be completely coated in a first processing step. In a second step, the coating must be removed from the electrodes and then the implant is folded at three folding lines for reducing the required area. Therefore, it is required that the coating is not only flexible but has a good adhesion to all the components. We expect that the adhesion between the coating (e.g. Parylene C) and the used material for the PCB-foil (DuPont Pyralux AP and insulating resist) might cause problems. This requires to change the substrate of the PCB-foil to something more suitable (e.g. Parylene C as well) and will hopefully give us the opportunity to reduce the thickness of the substrate for improving the bending radius of the PCB-foil. Currently, we are testing several promising candidates for coatings

and substrates [Tolstosheeva et al., 2013].

Another goal for the future is to add comprehensive stimulation capabilities to the implant for allowing electrical stimulation of the brain tissue (e.g. for visual cortical prostheses).

In summary, the actual state of the wireless module as well as the implant is not yet ready for implantation, especially not for long term implantation in medical applications. Several problems have to be solved in the future development. Nevertheless, we deliver an Open Hardware / Open Source tool kit containing PCB designs, FPGA firmwares, and software which allows interested researchers to develop their own wireless neuro-implant without starting from scratch for every component. Starting point for future developers will be a fully functional tool chain, starting with the software for controlling the implant and recording the measurement data, wireless power supply and telemetry, easily scalable number of analog front-ends and an adaptable application specific controller for the data processing on the implant.

Disclosure/Conflict-of-Interest Statement

The authors declare that the research was conducted in the absence of any commercial or financial relationships that could be construed as a potential conflict of interest.

Author Contributions

D.R. and J.P. wrote the paper. K.R.P. and D.R. intiated and supervised the research in this project. D.R., J.H., J.P., W.L., D.P.D., S.P., K.R.P. and A.K. developed the system concept. J.P. and J.H. prepared and conducted the test and startup. J.P. performed the measurements. J.P. and J.H. developed the ASIC. D.R. designed the PCBs and PCB-foil for the implant, the wireless module as well as the base station. D.R. wrote the firmwares for the basestation's FGPA and the nano FPGAs as well as the corresponding software package. D.B. worked on the wireless power transfer. S.P. provided the infrastructure for development, design and testing of the mixed signal circuitry. D.P.D. contributed the electronic design methodologies of the mixed signal circuitry. T.S. and M.S. developed the antennas. T.S., D.R., and M.S. created the corresponding antenna matching circuits. T.S. developed and built the energy harvesting coils. W.L. was responsible for the clean room technology. W.L. and E.T. contributed to the layout and realisation of electrodes. D.G. contributed to the tests of the base station.

Acknowledgement

We thank Norbert Hauser, Alexander Svojanovsky, and Mario Kaiser from Brain Products as well as Guido Widman and Christian Elger from the department of epileptology at the university hospital of Bonn for fruitfull discussions.

Funding This work was supported in part by Bundesministerium fuer Bildung und Forschung, Grant 01 EZ 0867 (Innovationswettbewerb Medizintechnik) and Grant 01 GQ 1106 (Bernstein Award Udo Ernst) as well as Research-Focus Neurotechnology University of Bremen, and the Creative Unit I-See 'The artifical eye: Chronic wireless interface to the visual cortex' at the University of Bremen.

Supplemental Data

In the supplemental data we present most of the design files for the firmwares, software and PCB designs as Open Source.

References

[Aceros et al., 2011] Aceros, J., Yin, M., Borton, D., Patterson, W., and Nurmikko, A. (2011). A 32-channel fully implantable wireless neurosensor for simultaneous recording from two cortical regions. *Annual International Conference of the IEEE Engineering in Medicine and Biology Society*, pages 2300–2306.

[Andersen et al., 2010] Andersen, R., Hwang, E., and Mulliken, G. (2010). Cognitive neural prosthetics. *Annu. Rev. Psychol.*, 61:169–190.

[Asgarian and Sodagar, 2011] Asgarian, F. and Sodagar, A. M. (2011). Wireless telemetry for implantable biomedical microsystems. *Biomedical Engineering, Trends in Electronics, Communications and Software*, pages 21–44.

[Aubert, 2011] Aubert, H. (2011). Rfid technology for human implant devices. *Comptes Rendus Physique*, 12.7:675–683.

[Barrese et al., 2013] Barrese, J. C., Rao, N., Paroo, K., Triebwasser, C., Vargas-Irwin, C., Franquemont, L., and Donoghue, J. P. (2013). Failure mode analysis of silicon-based intracortical microelectrode arrays in non-human primates. *Journal of Neural Engineering*, 10:066014.

[Borton et al., 2013] Borton, D. A., Yin, M., Aceros, J., and Nurmikko, A. (2013). An implantable wireless neural interface for recording cortical circuit dynamics in moving primates. *Journal of Neural Engineering*, 10(2):026010.

[Brunner et al., 2011] Brunner, P., Ritaccio, A., Emrich, J., Bischof, H., and Schalk, G. (2011). Rapid communication with a p300 matrix speller using electrocorticographic signals (ecog). *Front. Neurosci.*, 5:5:doi: 10.3389/fnins.2011.00005.

[Chae et al., 2009] Chae, M. S., Yang, Z., Yuce, M. R., Hoang, L., and Liu, W. (2009). A 128-channel 6 mw wireless neural recording ic with spike feature extraction and uwb transmitter. *Neural Systems and Rehabilitation Engineering, IEEE Transactions on*, 17(4):312–321.

[Charvet et al., 2013] Charvet, G., Sauter-Starace, F., M.Foerster, Ratel, D., Chabrol, C., Porcherot, J., Robinet, S., Reverdy, J., D'Errico, R., Mestais, C., and Benabid, A. (2013). Wimagine: 64-channel ecog recording implant for human applications. *Engineering in Medicine and Biology Society (EMBC), 2013 35th Annual International Conference of the IEEE*, pages 2756–2759.

[Dobelle, 1999] Dobelle, W. H. (1999). Artificial vision for the blind by connecting a television camera to the visual cortex. *ASAIO Journal (American Society for Artificial Internal Organs)*, 46.1:3–9.

[Harrison et al., 2009] Harrison, R. R., Kier, R. J., Chestek, C. A., Gilja, V., Nuyujukian, P., Ryu, S., Greger, B., Solzbacher, F., and Shenoy, K. V. (2009). Wireless neural recording with single low-power integrated circuit. *Rehabilitation*, 17(4):322–329.

[Harrison et al., 2008] Harrison, R. R., Kier, R. J., Kim, S., Rieth, L., Warren, D. J., Clark, N. M. L. G., Solzbacher, F., Chestek, C. A., Gilja, V., P.Nuyujukian, Ryu, S. I., and Shenoy, K. V. (2008). A wireless neural interface for chronic recording. *Biomedical Circuits and Systems Conference*, BioCAS 2008:125–128.

[Hirata et al., 2011] Hirata, M., Matsushita, K., Suzuki, T., Yoshida, T., Sato, F., Morris, S., Yanagisawa, T., Goto, T., Kawato, M., and Yoshimine, T. (2011). A fully-implantable wireless system for human brain-machine interfaces using brain surface electrodes: W-herbs. *IEICE TRANSACTIONS on Communications*, E94-B(9):2448–2453.

[Ho et al., 2014] Ho, J. S., Yeh, A. J., Neofytou, E., Kim, S., Tanabe, Y., Patlolla, B., Beygui, R. E., and Poon, A. S. Y. (2014). Wireless power transfer to deep-tissue microimplants. *PNAS*, 111(22):7974–7979.

[Hochberg et al., 2006] Hochberg, L., Serruya, M., Friehs, G., Mukand, J., Saleh, M., Caplan, A., Branner, A., Chen, D., Penn, R., and Donoghue, J. (2006). Neuronal ensemble control of prosthetic devices by a human with tetraplegia. *Nature*, 442:164–171.

[Hoeffmann et al., 2012] Hoeffmann, J., J.Pistor, Peters-Drolshagen, D., Tolstosheeva, E., Lang, W., and Paul, S. (2012). Biomedical-asic with reconfigurable data path for in vivo multi/micro-electrode recordings of bio-potentials. *MEA Meeting 2012*.

[IEEE, 2006] IEEE (2006). Ieee standard for safety levels with respect to human exposure to radio frequency electromagnetic fields, 3 khz to 300 ghz. *IEEE Standard for Safety Levels with Respect to Human Exposure to Radio Frequency Electromagnetic Fields, 3 kHz to 300 GHz*, page 98.

[Ifft et al., 2012] Ifft, R., Lebedev, M., and Nicolelis, M. (2012). Reprogramming movements: extraction of motor intentions from cortical ensemble activity when movement goals change. *Front Neuroeng.*, 5(16).

[Kim et al., 2009] Kim, S., Bhandari, R., Klein, M., Negi, S., Rieth, L., Tathireddy, P., Oppermann, M. T. H., and Solzbacher, F. (2009). Integrated wireless neural interface based on the utah electrode array. *Biomedical Microdevices*, 11(2):453–466.

[Kim et al., 2007a] Kim, S., Tathireddy, P., Normann, R. A., and Solzbacher, F. (2007a). In vitro and in vivo study of temperature increases in the brain due to a neural implant." neural engineering. *CNE'07*.

[Kim et al., 2007b] Kim, S., Tathireddy, P., Normann, R. A., and Solzbacher, F. (2007b). Thermal impact of an active 3-d microelectrode array implanted in the brain. *IEEE TRANSACTIONS ON NEURAL SYSTEMS AND REHABILITATION ENGINEERING*, 15(4):493–501.

[Lebedev and Nicolelis, 2006] Lebedev, M. and Nicolelis, M. (2006). Brain-machine interfaces: past, present and future. *Trends Neurosci.*, 29(9):536–546.

[Lebedev et al., 2011] Lebedev, M., Tate, A., Hanson, T., Z, Z. L., ODoherty, J., Winans, J., Ifft, P., Zhuang, K., Fitzsimmons, N., Schwarz, D., Fuller, A., An, J., and Nicolelis, M. (2011). Future developments in brain-machine interface research. *Clinics (Sao Paulo)*, 66(1):25–32.

[Lee et al., 2000] Lee, W. S., Lee, J. K., Lee, S. A., Kang, J. K., and Ko, T. S. (2000). Complications and results of subdural grid electrode implantation in epilepsy surgery. *Surg Neurol*, 54:346–351.

[Leuthardt et al., 2004] Leuthardt, E., Schalk, G., Wolpaw, J., Ojemann, J., and Moran, D. (2004). A braincomputer interface using electrocorticographic signals in humans. *Journal of Neural Engineering*, 1:63–71.

[Li et al., 2011] Li, Z., O'Doherty, J., Lebedev, M., and Nicolelis, M. (2011). Adaptive decoding for brain-machine interfaces through bayesian parameter updates. *Neural Comput.*, 23(12):3162–3204.

[Liu et al., 2009] Liu, Y.-H., Li, C.-L., and Lin, T.-H. (2009). A 200-pj/b mux-based rf transmitter for implantable multichannel neural recording. *IEEE Transactions on Microwave Theory and Techniques*, 57(10):2533–2541.

[Microsemi, 2010] Microsemi (2010). *ZL70102-Medical Implantable RF Transceiver MICS RF Telemetry*. Microsemi.

[Microsemi, 2013] Microsemi (2013). *ZL70120 MICS-Band RF Base Station Module (BSM)*. Microsemi. Rev. 4.

[Moran, 2010] Moran, D. (2010). Evolution of braincomputer interface: action potentials, local field potentials and electrocorticograms. *Current Opinion in Neurobiology*, 20(6):741–745.

[Muller et al., 2014] Muller, R., Hanh-Phuc, L., Wen, L., Ledochowitsch, P., Gambini, S., Bjorninen, T., Koralek, A., Carmena, J., Maharbiz, M., Alon, E., and Rabaey, J. (2014). 24.1 a miniaturized 64-channel 225µw wireless electrocorticographic neural sensor. *Solid-State Circuits Conference Digest of Technical Papers (ISSCC)*, pages 412–412.

[Musallam et al., 2004] Musallam, S., Corneil, B., Greger, B., Scherberger, H., and Andersen, R. (2004). Cognitive control signals for neural prosthetics. *Science*, 305:258–262.

[Nair et al., 2008] Nair, D. R., Burgess, R., McIntyre, C. C., and Lueders, H. (2008). Chronic subdural electrodes in the management of epilepsy. *Clinical Neurophysiology*, 119(1):11–28.

[Navaii et al., 2012] Navaii, M. L., Jalali, M., and Sadjedi, H. (2012). An ultra-low power rf interface for wireless-implantable microsystems. *Microelectronics Journal*, 43(11):848 – 856.

[NDK, 2013] NDK (2013). *NZ2016S Series - Crystal Clock Oscillator*. NDK.

[Olivo et al., 2011] Olivo, J., Carrara, S., and Micheli, G. D. (2011). Energy harvesting and remote powering for implantable biosensors. *IEEE SENSORS JOURNAL*, 11(7):1573.

[OrangeTreeTechnologies, 2013] OrangeTreeTechnologies (2013). *ZestET1: GigE TOE & FPGA Module*. Orange Tree Technologies.

[Pistohl et al., 2008] Pistohl, T., Ball, T., , A. S.-B., , Aertsen, A., and Mehring, C. (2008). Prediction of arm movement trajectories from ecog-recordings in humans. *Journal of Neuroscience Methods*, 167:105–114.

[Pistohl et al., 2012] Pistohl, T., Schulze-Bonhage, A., Aertsen, A., Mehring, C., and Ball, T. (2012). Decoding natural grasp types from human ecog. *NeuroImage*, 59:248–260.

[Pistor et al., 2011] Pistor, J., Hoeffmann, J., Peters-Drolshagen, D., and Paul, S. (2011). A programmable neural measurement system for spikes and local field potentials. *DTIP Aix-en-Provence*.

[Pistor et al., 2013] Pistor, J., Hoeffmann, J., Rotermund, D., Tolstosheeva, E., Schellenberg, T., Boll, D., Gordillo-Gonzalez, V., Mandon, S., Peters-Drolshagen, D., Kreiter, A. K., Schneider, M., Lang, W., Pawelzik, K. R., and Paul, S. (2013). Development of a fully implantable recording system for ecog signals. *Design, Automation and Test in Europe*.

[Rapoport et al., 2012] Rapoport, B. I., Kedzierski, J. T., and Sarpeshkar, R. (2012). A glucose fuel cell for implantable brainmachine interfaces. *PLoS ONE*, 7(6):e38436.

[RFMonolithics, 2010] RFMonolithics (2010). *RF2607D-403.5 MHz SAW Filter*. RF Monolithics, Inc.

[Rotermund et al., 2006] Rotermund, D., Ernst, U., and Pawelzik, K. (2006). Towards on-line adaptation of neuro-prostheses with neuronal evaluation signals. *Biological Cybernetics*, 95:243–257.

[Rotermund et al., 2013] Rotermund, D., Ernst, U. A., Mandon, S., Taylor, K., Smiyukha, Y., Kreiter, A. K., and Pawelzik, K. R. (2013). Toward high performance, weakly invasive brain computer interfaces using selective visual attention. *The Journal of Neuroscience*, 33(14):6001–6011.

[Schalk, 2010] Schalk, G. (2010). Can electrocorticography (ecog) support robust and powerful brain-computer interfaces? *Front Neuroengineering.*, 3:9.

[Schiller and Tehovnik, 2008] Schiller, P. H. and Tehovnik, E. J. (2008). Visual prosthesis. *Perception*, 37:1529–1559.

[Schmidt et al., 1996] Schmidt, E. M., Bak, M. J., Hambrecht, F. T., Kufta, C. V., O'Rourke, D., and Valiabhanath, P. (1996). Feasibility of a visual prosthesis for the blind based on intracortical microstimulation of the visual cortex. *Brain*, 119:507–522.

[Schwerdt et al., 2011] Schwerdt, H. N., Xu, W., Shekhar, S., Abbaspour-Tamijani, A., Towe, B. C., Miranda, F. A., and Chae, J. (2011). A fully-passive wireless microsystem for recording of neuropotentials using rf backscattering methods. *J Microelectromech Syst.*, 20(5):1119–1130.

[Sharma et al., 2011] Sharma, A., Rieth, L., Tathireddy, P., Harrison, R., Oppermann, H., Klein, M., Topper, M., Jung, E., Normann, R., Clark, G., and Solzbacher, F. (2011). Evaluation of the packaging and encapsulation reliability in fully integrated, fully wireless 100 channel utah slant electrode array (usea): Implications for long term functionality. *16th International Solid-State Sensors, Actuators and Microsystems Conference*, pages 1204–1207.

[Silay et al., 2008] Silay, K. M., Dehollain, C., and Declercq, M. (2008). Numerical analysis of temperature elevation in the head due to power dissipation in a cortical implant. *Engineering in Medicine and Biology Society*, 30th Annual International Conference of the IEEE.

[Simeral et al., 2011] Simeral, J., Kim, S.-P., Black, M., Donoghue, J., and Hochberg, L. R. (2011). Neural control of cursor trajectory and click by a human with tetraplegia 1000 days after implant of an intracortical microelectrode. *Journal of Neural Engineering*.

[TI, 2010] TI (2010). *bq25046EVM-687 Evaluation Module*. Texas Instruments. SLVU420.

[TI, 2011] TI (2011). *bqTESLA Portfolio of Wireless Power Solutions*. Texas Instruments.

[TI, 2012] TI (2012). *bq51013-Integrated Wireless Power Supply Receiver, Qi (Wireless Power Consortium) Compliant*. Texas Instruments. SLVSAT9D.

[Tolstosheeva et al., 2011] Tolstosheeva, E., Gordillo-Gonzalez, V., Hertzberg, T., Kempen, L., Michels, I., Kreiter, A., and Lang, W. (2011). A novel flex-rigid and soft-release ecog array. *33rd Annual International IEEE EMBS Conference*.

[Tolstosheeva et al., 2013] Tolstosheeva, E., Hoeffmann, J., Pistor, J., Rotermund, D., Schellenberg, T., Boll, D., Hertzberg, T., Gordillo-Gonzalez, V., Mandon, S., Peters-Drolshagen, D., Schneider, M., Pawelzik, K. R., Kreiter, A. K., Paul, S., and Lang, W. (2013). Towards a wireless and fully-implantable ecog system. *Transducers - The 17th International Conference on Solid-State Sensors, Actuators and Microsystems*, page M3P.095.

[Torex, 2011] Torex (2011). *XCL206-Inductor Built-in Step-Down micro DC/DC Converters*. Torex.

[van Gerven et al., 2009] van Gerven, M., Farquhar, J., Schaefer, R., Vlek, R., Geuze, J., Nijholt, A., Ramsey, N., Haselager, P., Vuurpijl, L., Gielen, S., and Desain, P. (2009). The braincomputer interface cycle. *Journal of Neural Engineering*, 6.

[Velliste et al., 2008] Velliste, M., Perel, S., Spalding, M., Whitford, A., and Schwartz, A. (2008). Cortical control of a prosthetic arm for self-feeding. *Nature*, 453:1098–1101.

[Voges et al., 2006] Voges, J., Waerzeggers, Y., Maarouf, M., Lehrke, R., Koulousakis, A., Lenartz, D., and Sturm, V. (2006). Deep-brain stimulation: long-term analysis of complications caused by hardware and surgery – experiences from a single centre. *J Neurol Neurosurg Psychiatry.*, 77(7):868–872.

[Wang et al., 2013] Wang, W., Collinger, J. L., Degenhart, A. D., Tyler-Kabara, E. C., Schwartz, A. B., Moran, D. W., Weber, D. J., Wodlinger, B., Vinjamuri, R. K., Ashmore, R. C., Kelly, J. W., and Boninger, M. L. (2013). An electrocorticographic brain interface in an individual with tetraplegia. *PloS one*, 8(2):e55344.

[WPC, 2014] WPC, W. P. C. (2014). Wpc to demo worlds most advanced resonant wireless charging system compatible with existing 40+ million qi phones.

[Wu and Hatsopoulos, 2008] Wu, W. and Hatsopoulos, N. (2008). Real-time decoding of nonstationary neural activity in motor cortex. *IEEE Trans Neural Syst Rehabil Eng.*, 16(3):213–222.

[Yin et al., 2012] Yin, M., Borton, D., Aceros, J., Patterson, W., and Nurmikko, A. V. (2012). A 100-channel hermetically sealed implantable device for wireless neurosensing applications. *Circuits and Systems (ISCAS)*, pages 2629–2632.

Figures

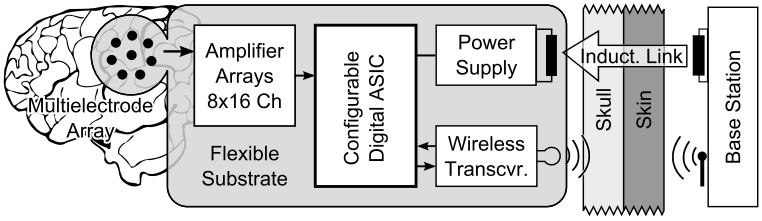

Figure 1. Concept of the implant with its base station.

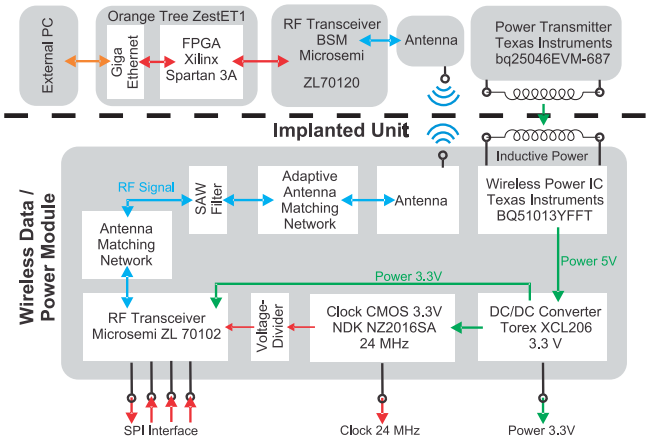

Figure 2. Overview of the components required for realizing the presented system concept of the wireless energy and data link.

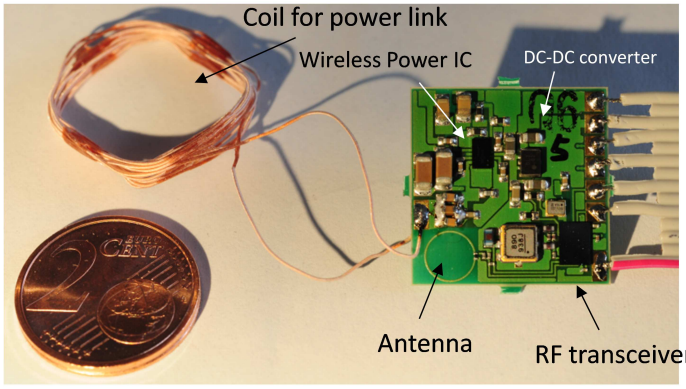

Figure 3. Realisation of the wireless data / power module on a 0.15mm thick FR4 board (20x20x1.6mm3) with its hand wound coil for the inductive power link.

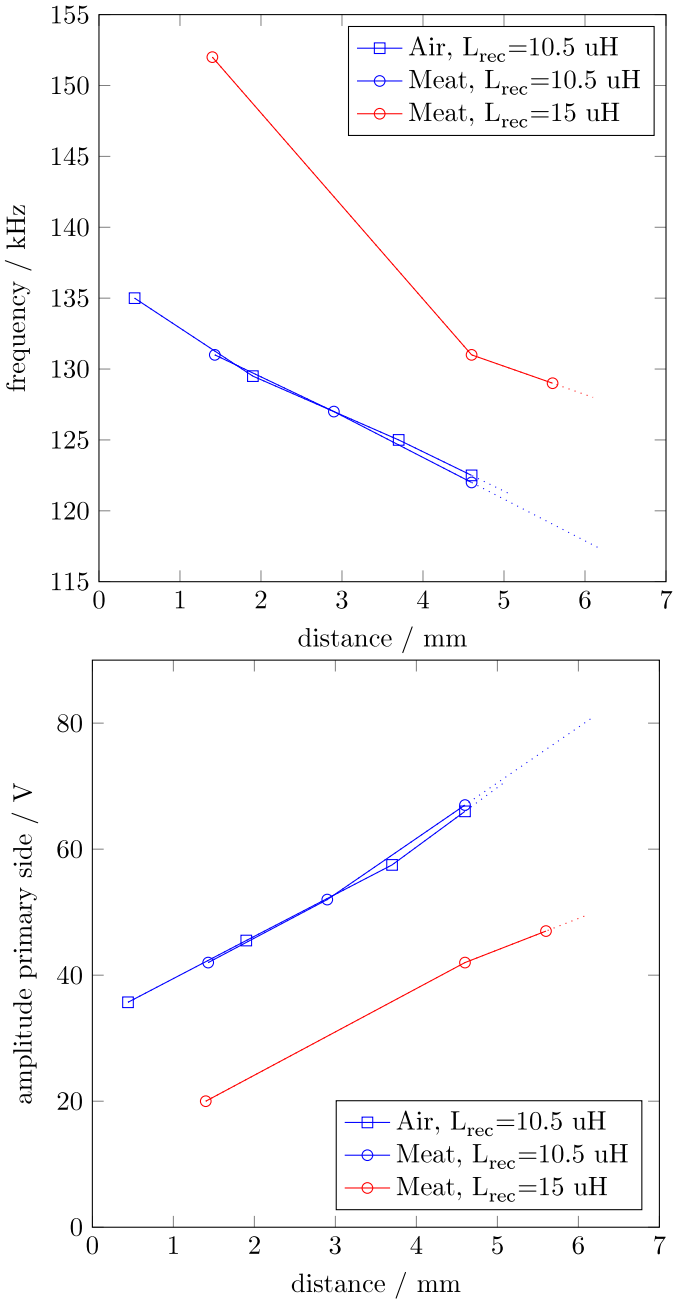

Figure 4. Wireless operation distances and according frequencies and primary voltages.

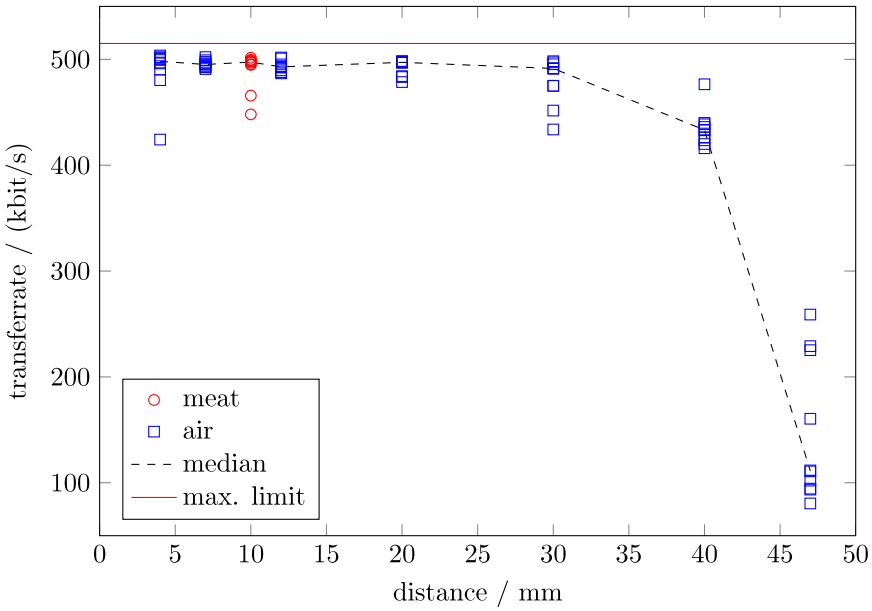

Figure 5. Data transfer rates for different distances.

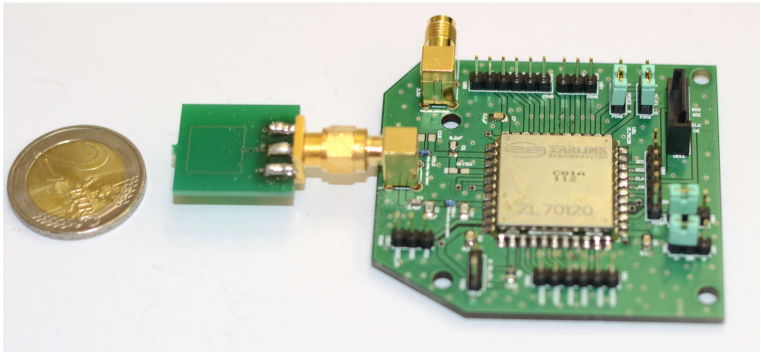

Figure 6. Base station RF transceiver module based on a Microsemi ZL70120 module and an in-house designed antenna. The rest of the base station has to be connected via SPI to this module.

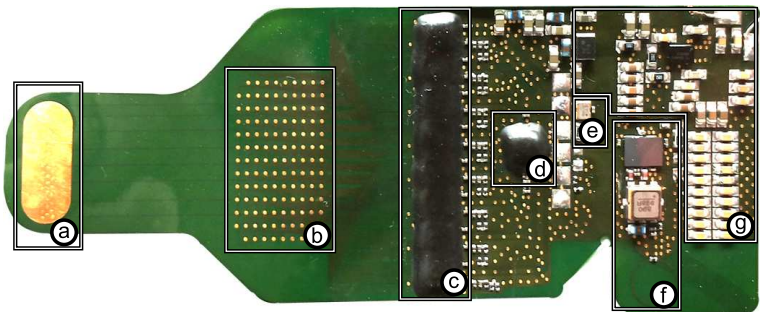

Figure 7. Implant prototype: (a) Reference electrode, (b) 128 electrodes, (c) 8xRHA, (d) ASIC, (e) 24 MHz clock, (f) RF-transceiver, (g) Inductive energy link

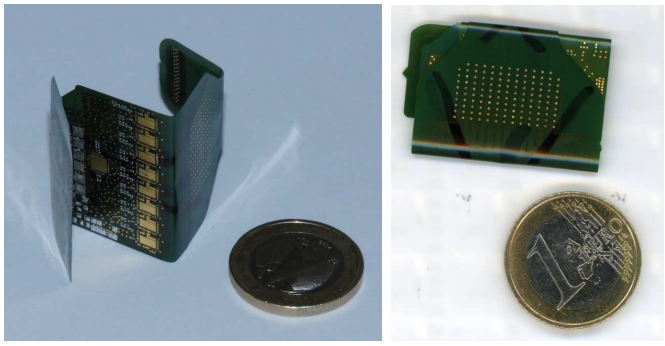

Figure 8. The implant is based on a flexible substrate, which allows it to be folded along three axes. This reduces the required space for implantation

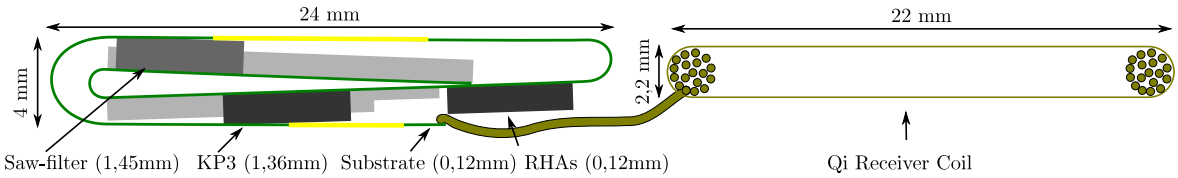

Figure 9. Kalomed Prototype with bending radius of 0.64mm (left) and coil for power supply (right)

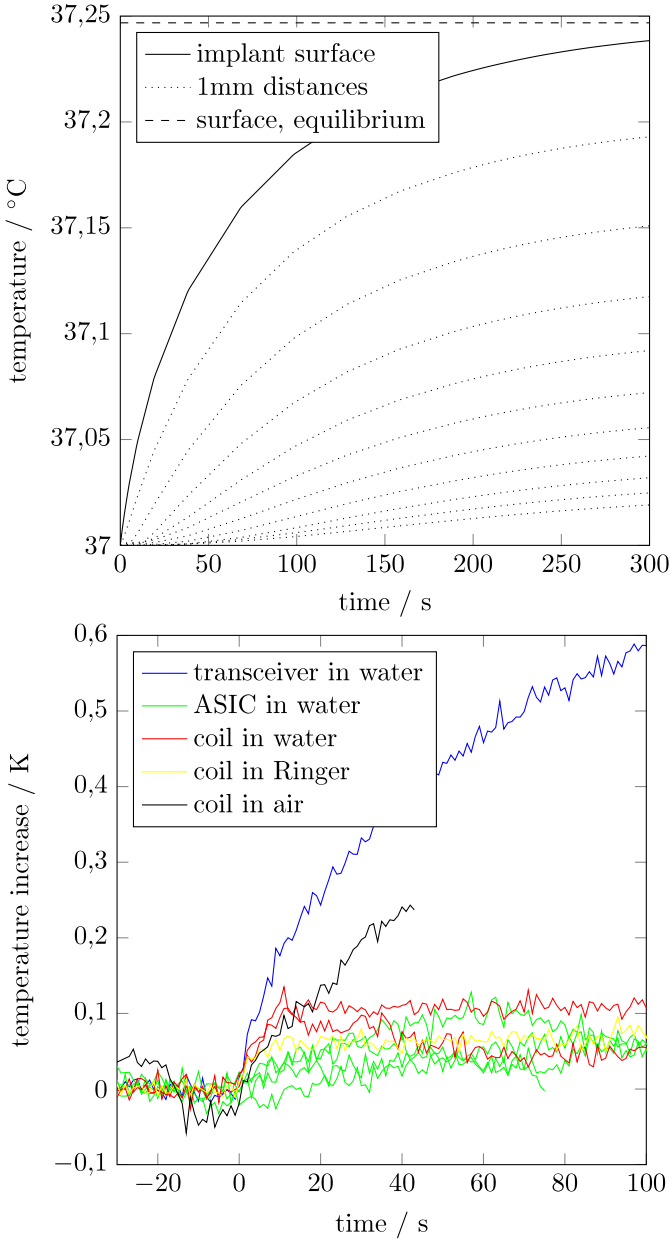

Figure 10. Left: Simulated heatup. Right: Measured temperature increase after power on.

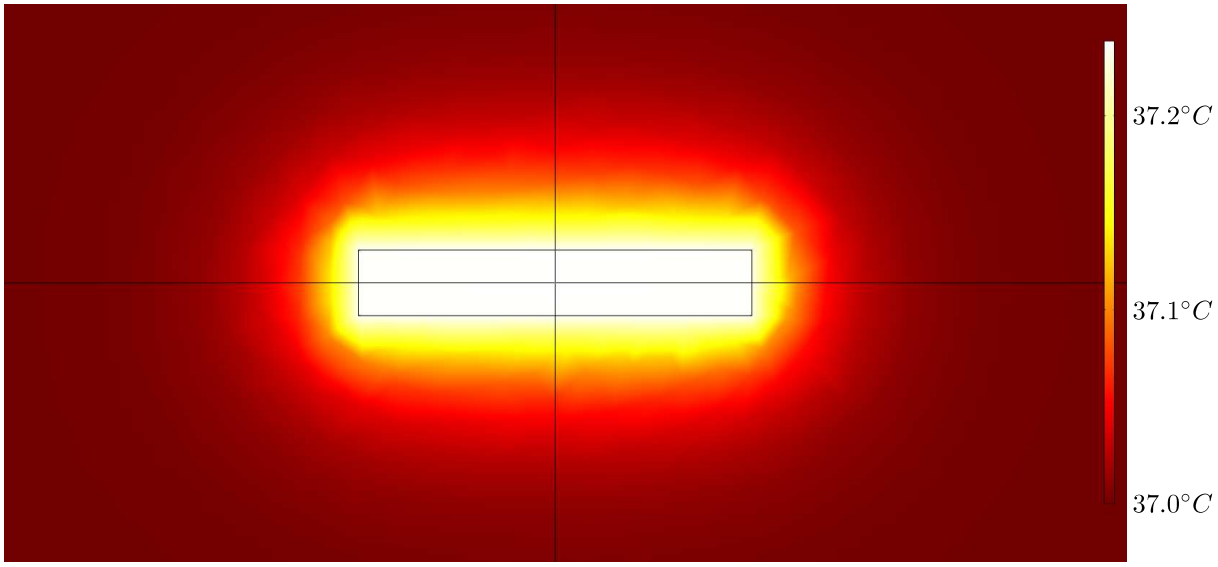

Figure 11. Temperature distribution after 300 seconds, caclulated with a simple FEM model (COMSOL). Rectangle shows the 24mm x 4mm implant cross section dimensions.

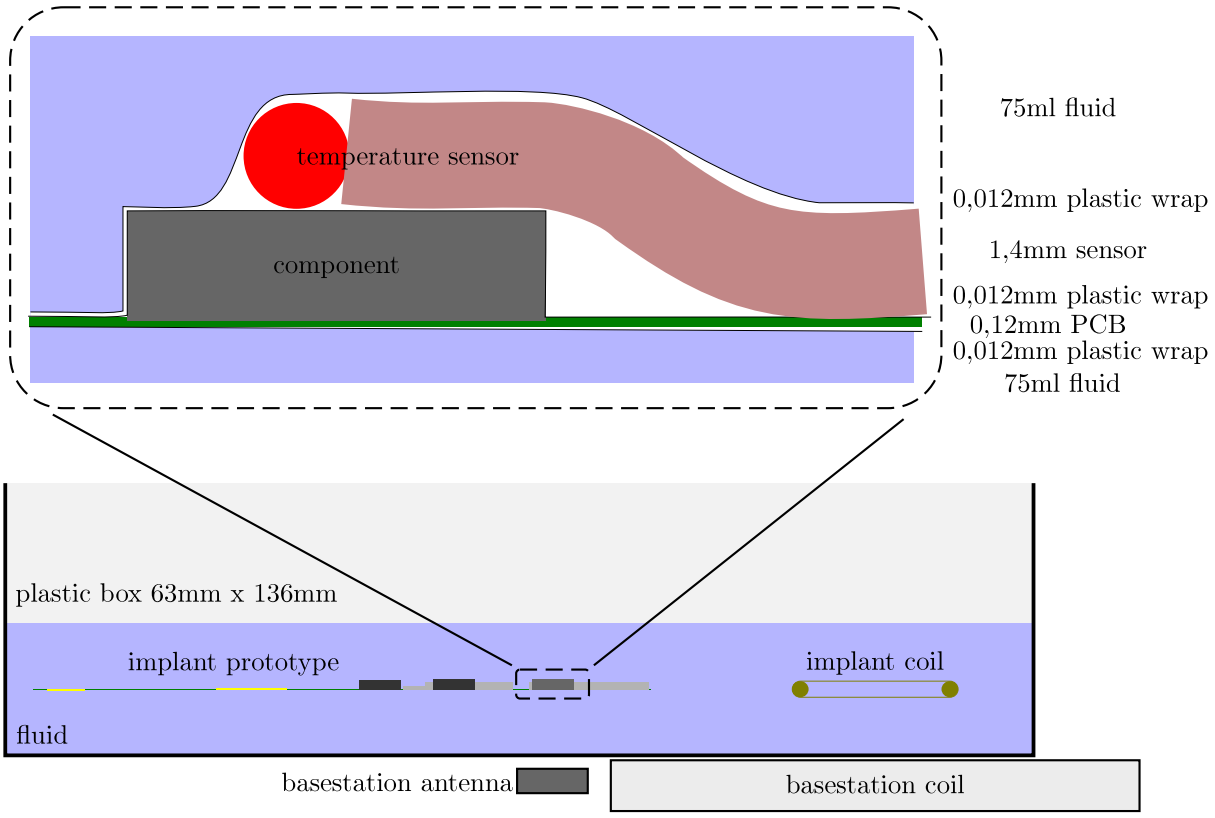

Figure 12. Measurement Setup for Heatup Test.

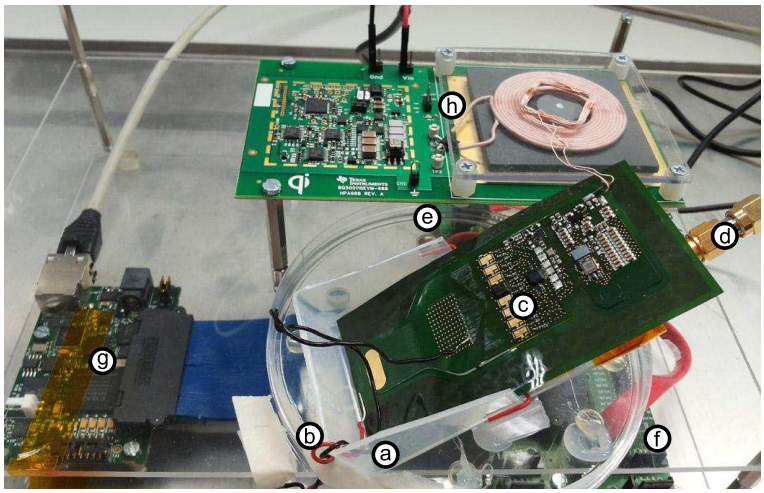

Figure 13. The complete system and measurement setup. A plastic box (a) is filled with Ringers Solution to simulate the fluids of the brain. The red and the black wire (b) are dipped into the fluid to apply a test stimulus between the electrodes and the reference electrode of the implant prototype (c). Underneath the implant lies the receiver antenna which is connected (d) to the base station receiver board (e). An adapter board (f) connects the receiver to the base station FPGA board (Orange Tree Zest ET1) (g), which provides the data via Ethernet. The implant is powered using the TI bq25046EVM-687 kit board (e).

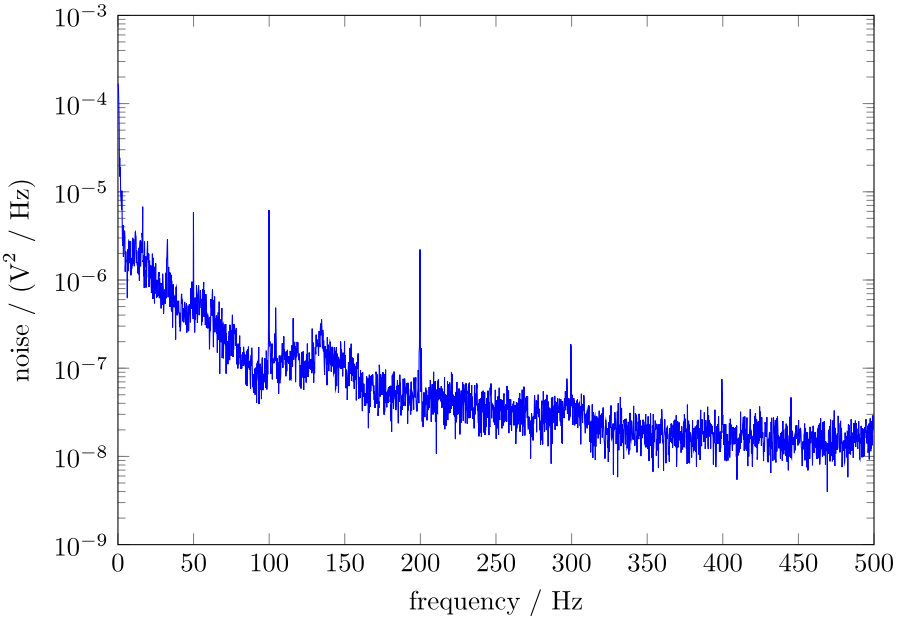

Figure 14. Noise spectrum for open inputs in Ringer solution.

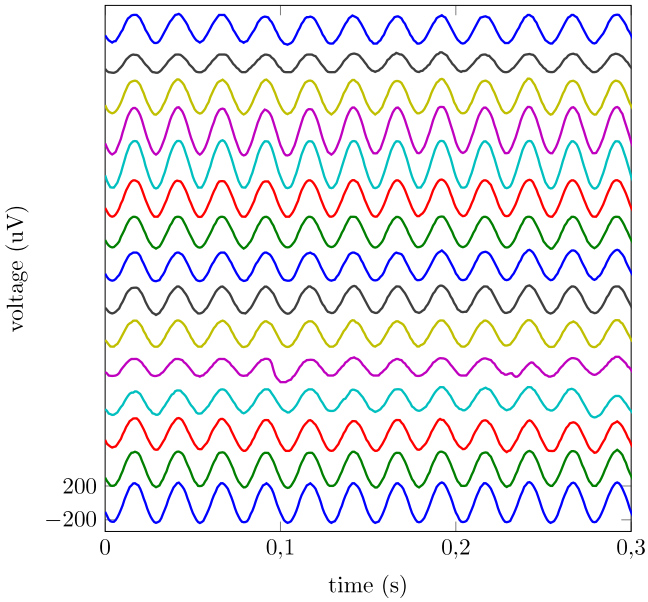

Figure 15. Received signals for a 40 Hz test signal. The amplitude depends on the distance between the stimulating wire and the channel electrode. The different channels are depicted in offset steps of 400 µV.